ITERATIVE ESTIMATION OF SIGNAL PARAMETERS USING FAST RECURSIVE 3D-ESPRIT

Tadaaki KURODA Nobuyoshi KIKUMA Naoki INAGAKI
Department of Electrical and Computer Engineering
Nagoya Institute of Technology
Gokiso-cho, Showa-ku, Nagoya 466-8555, Japan
E-mail: tadaaki@maxwell.elcom.nitech.ac.jp

1 Introduction

Many array signal processing techniques have been proposed for application in not only mobile communication systems but also intelligent transport systems[1]. Particularly, much attention is now focused on adaptive and signal processing antenna arrays operating in the spatial domain[2]. In general, mobile radio propagation is characterized by strong multipath effects, so multipath fading deteriorates the quality of digital communications. In order to understand the multipath wave propagation structures, it is most effective to estimate the signal parameters (DOA and TOA etc.) of the individual incoming waves. Further, utilizing the estimated information, we can form easily optimum beam patterns of antenna arrays in the mobile radio environments.

Recently, the ESPRIT algorithm receives our great interest because of its high resolution and high computational efficiency in estimating the signal parameters[3][4]. However, the conventional ESPRIT algorithm is not devised essentially for the real-time and on-line signal processing. Besides, in pairing the multiple signal parameters obtained from the multi-dimensional ESPRIT[5], we have to rely on somewhat complicated schemes such as the simultaneous Schur decomposition (SSD)[5].

In this paper, therefore, we will extend the fast recursive ESPRIT (1D)[7] to the fast recursive 3D-ESPRIT that updates the 2D-DOA(azimuth and elevation angles) and TOA information at each time instant, depending on the new data snapshot from a planar antenna array and frequency sweep operation. The recursive 3D-ESPRIT presented herein is based on the Standard ESPRIT and the BiSVD subspace tracking method involving QR-decomposition[6][7]. Also, this algorithm features utilizing the mean eigenvalue decomposition (MEVD) method[8] as the pairing procedure, which is much simpler than the SSD. Some computer simulation results will be shown to discuss and demonstrate the effectiveness of the proposed algorithm in terms of estimation accuracy and computation time.

2 Receiving System and Signal Models

Figure 1 shows the rectangular antenna array with $M_1 \times M_2$ identical antenna elements placed in the x-y plane. The element spacing is Δx and Δy in the x-axis and y-axis, respectively. In each element, the discrete frequency sweeping with the frequency step Δf is carried out and thus M_3-element frequency domain linear array data are obtained. Therefore, supposing the frequency domain is along the z-axis, we can regard the receiving system as a 3D-virtual rectangular array with $M_1 \times M_2 \times M_3 (\equiv M)$ elements. Also, it is assumed that L multipath waves with delay times τ_i $(i = 1, 2, ..., L)$ respectively are incident on the array and their 2D-DOAs(ϕ_i, θ_i: $i = 1, 2, ..., L$) are given in Fig.2.

In this situation, the data matrix at t time instant $\boldsymbol{X}(t)$ is defined by

$$\boldsymbol{X}(t) \triangleq \left[\begin{array}{cc} \alpha^{1/2}\boldsymbol{X}(t-1) & (1-\alpha)^{1/2}\boldsymbol{x}(t) \end{array} \right] \qquad (t = 1, 2, \cdots) \tag{1}$$

where $\boldsymbol{x}(t) \in C^{M\times 1}$ is the array snapshot vector at t time instant and $\alpha(0 < \alpha < 1)$ is the forgetting factor.

3 Principle of Fast Recursive 3D-ESPRIT

3.1 BiSVD subspace tracking method

Bi-Iteration SVD (BiSVD) subspace tracking method[6] is an algorithm of updating SVD of array data matrix iteratively and estimating recursively the signal subspace eigenvector matrix $\boldsymbol{Q}_A \in C^{M\times L}$ which is utilized in 3D-ESPRIT. $\boldsymbol{Q}_A(t)$ can be updated by the following equation [6].

$$\boldsymbol{Q}_A(t) = \boldsymbol{Q}_A(t-1)\boldsymbol{\Theta}_A(t) + \bar{\boldsymbol{x}}_\perp(t)\boldsymbol{f}^H(t) \tag{2}$$

$$\begin{array}{rclrcl}\bar{\boldsymbol{x}}_{\perp}(t) & \triangleq & n_x^{-1/2}(t)\boldsymbol{x}_{\perp}(t)\,, & \boldsymbol{x}_{\perp}(t) & \triangleq & \boldsymbol{x}(t)-\boldsymbol{Q}_A(t-1)\boldsymbol{h}(t) \\ n_x(t) & \triangleq & \boldsymbol{x}_{\perp}^H(t)\boldsymbol{x}_{\perp}(t)\,, & \boldsymbol{h}(t) & \triangleq & \boldsymbol{Q}_A^H(t-1)\boldsymbol{x}(t)\end{array} \tag{3}$$

$\boldsymbol{\Theta}_A(t)$ and $\boldsymbol{f}^H(t)$ in (2) are extracted from a certain matrix as follows:

$$\boldsymbol{G}_A^H(t) = \begin{array}{r}L\left\{\vphantom{\begin{array}{c}a\\a\end{array}}\right.\\ \end{array}\overbrace{\phantom{\boldsymbol{\Theta}_A(t)}}^{L}\!\!\!\!\!\!\!\!\!\!\!\!\!\!\!\left[\begin{array}{c|c}\boldsymbol{\Theta}_A(t) & * \\ \hline \boldsymbol{f}^H(t) & *\end{array}\right]\left.\vphantom{\begin{array}{c}a\\a\\a\end{array}}\right\} L+1$$

where "$*$" stands for uninteresting quantities and $\boldsymbol{G}_A^H(t)$ is an orthogonal matrix that is obtained from the QR-decomposition expressed in (4).

$$\boldsymbol{G}_A^H(t)\begin{bmatrix}\boldsymbol{R}_A(t)\\ 0\cdots 0\end{bmatrix} = \begin{bmatrix}\alpha\boldsymbol{R}_A(t-1)\boldsymbol{H}_R(t)+(1-\alpha)\boldsymbol{h}(t)\boldsymbol{h}_R^H(t)\\ (1-\alpha)n_x^{1/2}(t)\boldsymbol{h}_R^H(t)\end{bmatrix} \tag{4}$$

$$\boldsymbol{H}_R(t) \triangleq \boldsymbol{H}(t)\boldsymbol{R}_B^{-1}(t) \tag{5}$$

$$\boldsymbol{H}(t) \triangleq \boldsymbol{R}_B(t-1)\boldsymbol{\Theta}_A(t-1) \tag{6}$$

$$\boldsymbol{h}_R^H(t) \triangleq \boldsymbol{h}^H(t)\boldsymbol{R}_B^{-1}(t) \tag{7}$$

In the above equations, $\boldsymbol{R}_A(t)$ and $\boldsymbol{R}_B(t)$ are $L\times L$ upper triangular matrices. $\boldsymbol{R}_A(t)$ is updated by (4) and $\boldsymbol{R}_B(t)$ is updated by the following QR-decomposition.

$$\boldsymbol{G}_B^H(t)\begin{bmatrix}\boldsymbol{R}_B(t)\\ 0\cdots 0\end{bmatrix} = \begin{bmatrix}\alpha^{1/2}\boldsymbol{H}(t)\\ (1-\alpha)^{1/2}\boldsymbol{h}^H(t)\end{bmatrix} \tag{8}$$

$$\Big(\boldsymbol{G}_B^H(t) : \text{orthogonal matrix produced by QRD}\Big)$$

In this paper, the initial values are given by

$$\boldsymbol{Q}_A(0) = \begin{bmatrix}p\boldsymbol{I}_L\\ \boldsymbol{0}\end{bmatrix}\ (p\text{: constant}),\ \boldsymbol{R}_B(0)=\boldsymbol{\Theta}_A(0)=\boldsymbol{I}_L\,,\ \boldsymbol{R}_A(0)=\boldsymbol{0}_{L\times L} \tag{9}$$

on the assumption that L is known or estimated by another method such as Akaike Information Criteria (AIC) or Minimum Description Length (MDL)[6].

3.2 Recursive 3D-ESPRIT

The recursive 3D-ESPRIT[7] is a QRD-based 3-dimensional ESPRIT algorithm of updating recursively the matrices $\boldsymbol{\Psi}_1(t)$, $\boldsymbol{\Psi}_2(t)$ and $\boldsymbol{\Psi}_3(t)$ that are derived from applying the rotational invariance[3] to the signal subspace eigenvector matrix provided by the above BiSVD subspace tracking method. In this stage, the same technique as the BiSVD is used for the QR-decomposition of coefficient matrices in getting $\boldsymbol{\Psi}_r(t)$ $(r=1,2,3)$ via linear equations like $\boldsymbol{A}\boldsymbol{\Psi}_r(t)=\boldsymbol{B}$[4]. $\boldsymbol{\Psi}_r(t)$ $(r=1,2,3)$ obtained in this way have following eigenstructures[4]:

$$\boldsymbol{\Psi}_r(t) = \boldsymbol{T}^{-1}(t)\boldsymbol{\Phi}_r(t)\boldsymbol{T}(t) \quad (r=1,2,3) \tag{10}$$

where $\boldsymbol{T}^{-1}(t)$ is an eigenvector matrix and $\boldsymbol{\Phi}_r(t)$ is a diagonal eigenvalue matrix of $\boldsymbol{\Psi}_r(t)$. The eigenvalue matrices $\boldsymbol{\Phi}_1(t)$, $\boldsymbol{\Phi}_2(t)$ and $\boldsymbol{\Phi}_3(t)$ include the signal parameters of the incident waves.

4 Mean Eigenvalue Decomposition(MEVD) Method

In 3D-ESPRIT, the estimated signal parameters must be paired signal by signal. In this paper, we employ the MEVD[8] to pair ϕ_i, θ_i and τ_i for the ith incident wave. From (10) , $\boldsymbol{\Psi}_1(t)$, $\boldsymbol{\Psi}_2(t)$ and $\boldsymbol{\Psi}_3(t)$ are found to have the common eigenvector, and so they have the following relationship.

$$\boldsymbol{\Psi}_1(t)+\boldsymbol{\Psi}_2(t)+\boldsymbol{\Psi}_3(t) = \boldsymbol{T}^{-1}(T)\left\{\boldsymbol{\Phi}_1(t)+\boldsymbol{\Phi}_2(t)+\boldsymbol{\Phi}_3(t)\right\}\boldsymbol{T}(t) \tag{11}$$

Therefore, after calculating the common eigenvector $\boldsymbol{T}^{-1}(t)$ of (11), we can obtain the eigenvalues of $\boldsymbol{\Psi}_1(t)$, $\boldsymbol{\Psi}_2(t)$ and $\boldsymbol{\Psi}_3(t)$ as follows:

$$\boldsymbol{\Phi}_r(t) = \boldsymbol{T}(t)\boldsymbol{\Psi}_r(t)\boldsymbol{T}^{-1}(t) \quad (r=1,2,3). \tag{12}$$

This is the MEVD providing the paired signal parameters (ϕ_i,θ_i,τ_i) of all waves[8].

5 Computer Simulation

In this section, computer simulation is carried out using $2 \times 2 \quad (M_1 = M_2 = 2)$ rectangular array of isotropic elements with an element spacing of a half wavelength. The center frequency is 5.2GHz, the frequency sweep width is 200MHz, and the number of frequency data is $11(M_3 = 11)$. There are two multipath waves arriving at the array $(L = 2)$, and they are completely correlated with each other. The Gaussian internal noises (thermal noises) of equal power exist at all antenna elements, and they are statistically independent of incident waves. Detail of a radio environment is described in Table 1. To decorrelate the coherent waves, the spatial smoothing processing (SSP)[9] is incorporated into our algorithm. In this simulation, the control parameter p which gives the initial value of $\boldsymbol{Q}_A(t)$ is 10^{-8}, and the forgetting factor α is 0.85. Also, SNR is 20dB and the subarray size for the SSP is $2 \times 2 \times 7$.

RMSEs of estimates for each wave are computed from 100 independent trials and used for sample performance statics. Figures 3 to 5 show the time variation of RMSEs for wave 1. For comparison, the estimation results by the conventional TLS-ESPRIT estimator (Standard ESPRIT with MEVD) are plotted in the same figures. It is found from the figures that RMSEs of TLS-ESPRIT are better than those of the recursive ESPRIT. However, the difference between them is much small and so we can say the recursive ESPRIT also provides accurate estimation. The results for wave 2 are the same as wave 1 although they are not shown here.

Further, we measured the computation time of the proposed estimator and the TLS-ESPRIT estimator. Figure 6 shows the computation time for one update. Obviously, the computation time of the TLS-ESPRIT increases as the number of elements grows large, while the recursive ESPRIT preserves almost constant and less computational load.

6 Conclusion

In this paper, we have developed the QRD-based fast recursive 3D-ESPRIT for estimating 2D-DOA and TOA of the multipath waves. Via computer simulation, we have shown that the proposed algorithm is effective enough in estimation accuracy and computation time. The successful results enable us to use the proposed algorithm as the real-time processor in the mobile radio systems.

References

[1] Y.Ogawa and N.Kikuma: "High-Resolution Techniques in Signal Processing Antennas," IEICE Trans. Commun., Vol.E78-B, No.11, pp.1435–1442, Nov. 1995.

[2] J.C.Liberty, JR. and T.S.Rappaport: *Smart Antennas for Wireless Communications: IS-95 and Third Generation CDMA Applications*, Prentice Hall, Inc., 1999.

[3] R.Roy and T.Kailath: "ESPRIT – Estimation of Signal Parameters via Rotational Invariance Techniques," IEEE Trans., Vol.ASSP-37, No.7, pp.984–995, July 1989.

[4] B.Ottersten, M.Viberg and T.Kailath: "Performance Analysis of the Total Least Squares ESPRIT Algorithm," IEEE Trans. on Signal Processing, Vol.39, No.5, pp.1122–1135, May. 1991.

[5] M.Haardt and J.A.Nossek: "Simultaneous Schur Decomposition of Several Nonsymmetric Matrices to Achieve Automatic Pairing in Multidimensional Harmonic Retrieval Problems," IEEE Trans. Signal Processing, Vol.46, No.1, pp.161–169, Jan. 1998.

[6] Peter Strobach : " Bi-iteration SVD subspace tracking algorithms and applications," IEEE Trans. Signal Processing, Vol.45, No.5, pp.1222-1240, May 1997.

[7] Peter Strobach: "Fast recursive subspace adaptive ESPRIT algorithms," IEEE Trans. Signal Processing, Vol.46, No.9, pp.2413–2430, Sept. 1998.

[8] N.Kikuma, H.Kikuchi, and N.Inagaki: "Pairing of Estimates Using Mean Eigenvalue Decomposition in Multi-Dimensional Unitary ESPRIT," IEICE Trans., Vol.J82-B, No.11, pp.2202–2207, Nov. 1999.

[9] T.J Shan, et al.: "On Spatial Smoothing for Direction-of-Arrival Estimation of Coherent Signals," IEEE Trans., Vol.ASSP-33, No.8, pp.806–811, Aug. 1985.

Table 1: Radio environment

	θ[deg]	ϕ[deg]	τ[ns]	power[dB]
wave 1	30→45	30→45	0→0	0
wave 2	50→60	50→60	10→5	0

(Angles and delay times are changed at the 100th sample.)

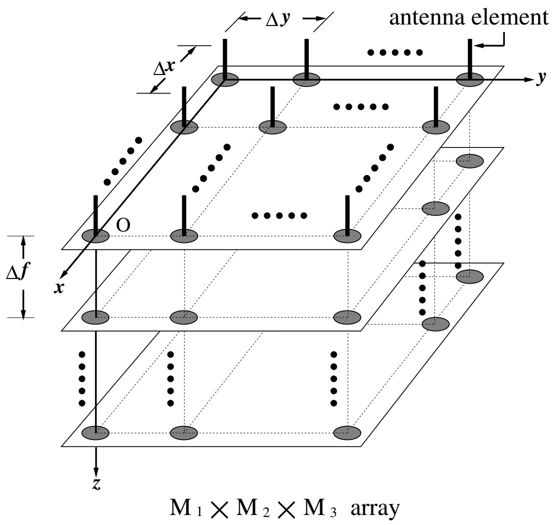

Figure 1: 3D virtual rectangular array

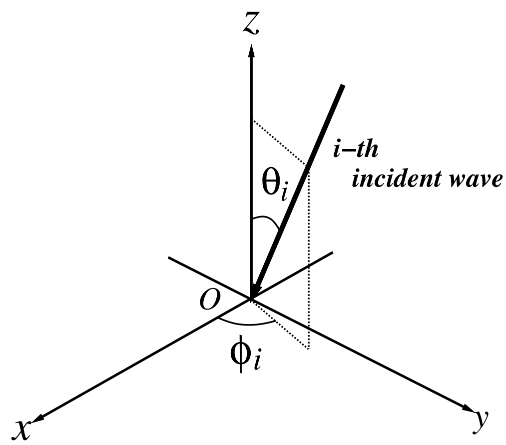

Figure 2: 2D-DOA of incident wave

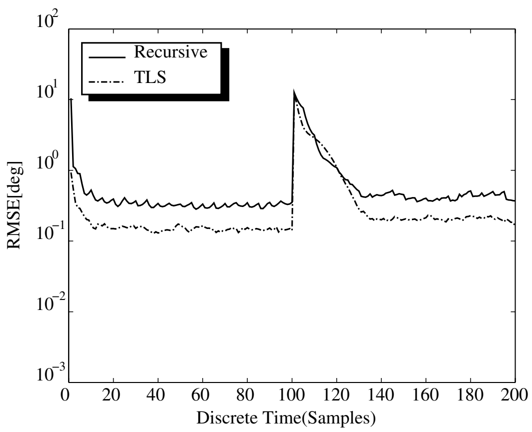

Figure 3: RMSE versus discrete time (samples) [elevation angle of wave 1]

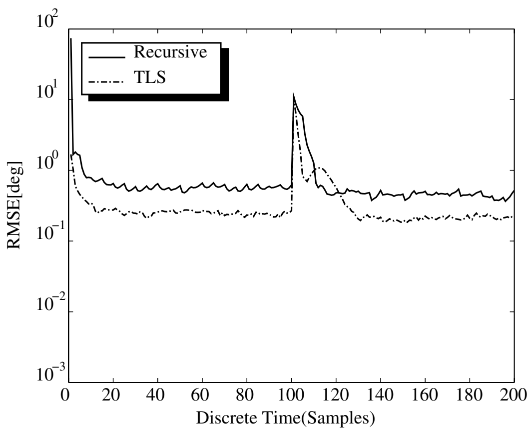

Figure 4: RMSE versus discrete time (samples) [azimuth angle of wave 1]

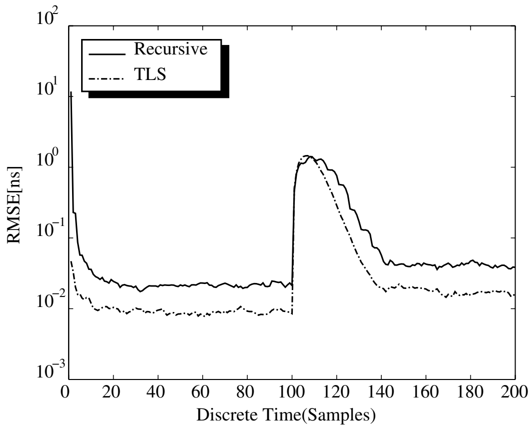

Figure 5: RMSE versus discrete time (samples) [delay time of wave 1]

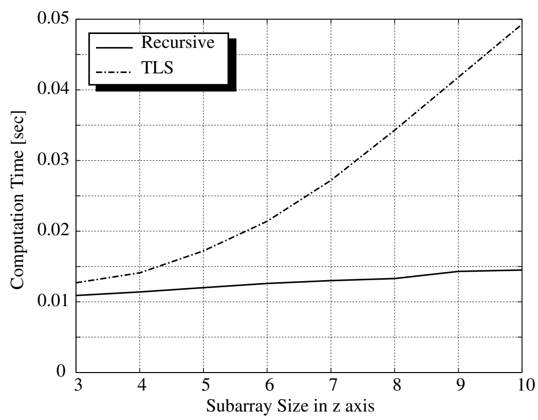

Figure 6: Computation time for one update as a function of M_3 in case $M_1 = M_2 = 2$